ETHYLENE RESPONSE FACTOR070 Regulates Root Development and Phosphate Starvation-Mediated Responses[1][C][W][OPEN]

Madhuvanthi Ramaiah, Ajay Jain, and Kashchandra G. Raghothama*

Department of Horticulture and Landscape Architecture, Purdue University, West Lafayette, Indiana 47907–1165 (M.R., K.G.R.); and National Research Centre on Plant Biotechnology, Pusa Campus, New Delhi 110012, India (A.J.)

Inorganic phosphate (Pi) availability is a major factor determining growth and consequently the productivity of crops. However, it is one of the least available macronutrients due to its high fixation in the rhizospheres. To overcome this constraint, plants have developed adaptive responses to better acquire, utilize, and recycle Pi. Molecular determinants of these adaptive mechanisms include transcription factors (TFs) that play a major role in transcriptional control, thereby regulating genome-scale networks. In this study, we have characterized the biological role of *Arabidopsis thaliana Ethylene Response Factor070* (*AtERF070*), a Pi starvation-induced TF belonging to the APETALA2/ETHYLENE RESPONSE FACTOR family of TFs in Arabidopsis (*Arabidopsis thaliana*). It is localized to the nucleus and induced specifically in Pi-deprived roots and shoots. RNA interference-mediated suppression of *AtERF070* led to augmented lateral root development resulting in higher Pi accumulation, whereas there were reductions in both primary root length and lateral root number in 12-d-old transgenic seedlings overexpressing *AtERF070*. When the overexpressing lines were grown to maturity under greenhouse conditions, they revealed a stunted bushy appearance that could be rescued by gibberellic acid application. Furthermore, a number of Pi starvation-responsive genes were modulated in *AtERF070*-overexpressing and RNA interference lines, thereby suggesting a potential role for this TF in maintaining Pi homeostasis.

Inorganic phosphate (Pi) is one of the essential macronutrients that plays a pivotal role in metabolic processes (Marschner, 1995). Despite high Pi content in natural and agroclimatic environments, its availability is limited by its high fixation and slow diffusion rates in rhizospheres (Raghothama, 1999; Plaxton and Tran, 2011). Plants adapt to Pi deficiency by evolving an array of developmental, biochemical, and molecular responses facilitating optimal acquisition, mobilization, and distribution of Pi (Franco-Zorrilla et al., 2004; Lynch, 2011; Smith et al., 2011; Jain et al., 2012). In Arabidopsis (*Arabidopsis thaliana*), Pi deficiency triggers modulation of root system architecture (RSA), and increases in the number and length of root hairs, thereby enabling plants to acquire Pi from soils (Bates and Lynch, 1996; Ma et al., 2001; Williamson et al., 2001; López-Bucio et al., 2002; Jain et al., 2007b, 2012). In addition, increased production of phosphatases and RNases and activation of alternative nonphosphorylating metabolic pathways further facilitate the adaptation to limited Pi availability (López-Bucio et al., 2002; Rausch and Bucher, 2002; Vance et al., 2003; Hammond et al., 2004; Plaxton and Tran, 2011). Global gene expression analyses using microarrays have resulted in the identification of several Pi starvation-responsive (PSR) genes that are implicated in Pi homeostasis (Misson et al., 2005; Morcuende et al., 2007; Müller et al., 2007; Calderon-Vazquez et al., 2008; Thibaud et al., 2010). In addition, developmental and molecular changes during Pi starvation are mediated by phytohormones like auxin, cytokinin, ethylene, and GA_3 (Franco-Zorrilla et al., 2004; Jain et al., 2007a; Jiang et al., 2007; O'Rourke et al., 2013).

In Arabidopsis, transcriptional regulation of Pi-deficiency responses involves an array of transcription factors (TFs; *PHOSPHATE STARVATION RESPONSE1* [*PHR1*, At4g28610], *PHOSPHATE STARVATION RESPONSE1-LIKE1* [*PHR1-like1*, At5g29000], *PHOSPHATE ROOT DEVELOPMENT* [*PRD*, At1g79700], *BASIC HELIX-LOOP-HELIX32* [*bHLH32*, At3g25710], *WRKY6* [At1g62300], *HYPERSENSITIVITY TO LOW PHOSPHATE-ELICITED PRIMARY ROOT SHORTENING1* [*HRS1*, At1g13300], *WRKY75* [At5g13080], *ZINC FINGER OF ARABIDOPSIS6* [*ZAT6*, At5g04340], *MYB62* and *MYB DOMAIN PROTEIN62* [*MYB62*, At1g68320]) that have been functionally characterized (Rubio et al., 2001; Chen et al., 2007, 2009; Devaiah et al., 2007a, 2007b, 2009; Liu et al., 2009; Bustos et al., 2010). Among these TFs, extensively studied *PHR1* has been implicated in regulating a subset of Pi-starvation responses, in spite of not being induced during Pi deficiency. To identify PSR genes that are implicated in

[1] This work was supported by the McKnight Foundation (grants to K.G.R.) and by the Ministry of Science and Technology, Department of Biotechnology, Government of India (Ramalingaswamy Fellowship [BT/HRD/35/02/26/2009] to A.J.).

* Address correspondence to kraghoth@purdue.edu.

The author responsible for distribution of materials integral to the findings presented in this article in accordance with the policy described in the Instructions for Authors (www.plantphysiol.org) is: Kashchandra G. Raghothama (kraghoth@purdue.edu).

[C] Some figures in this article are displayed in color online but in black and white in the print edition.

[W] The online version of this article contains Web-only data.

[OPEN] Articles can be viewed online without a subscription.

www.plantphysiol.org/cgi/doi/10.1104/pp.113.231183

transcriptional regulation, a microarray analysis using Affymetrix was carried out by subjecting Arabidopsis to short-term (3, 6, and 12 h pooled), medium-term (1 and 2 d pooled), and long-term (10 d) Pi starvation (Misson et al., 2005). A total of 866 genes were found to be spatiotemporally and differentially regulated, of which 80 were involved in transcriptional regulation and some of them belonged to APETALA2, WRKY, BASIC REGION/LEUCINE ZIPPER MOTIF, MYB, and Zinc Finger superfamilies (Misson et al., 2005). *MYB62* and *ZAT6*, which showed induction only during long-term Pi deprivation in the leaf, have been functionally characterized (Misson et al., 2005; Devaiah et al., 2007b, 2009). The overexpression of *ZAT6* resulted in the suppression of PSR genes and alteration of RSA (Devaiah et al., 2007b), whereas overexpression of *MYB62* resulted in modulated RSA, elevated Pi uptake and acid phosphatase activity, attenuation in the expression of PSR genes, and an interaction with GA signaling pathway (Devaiah et al., 2009). These studies suggested that *MYB62* and *ZAT6* play critical roles in the maintenance of Pi homeostasis. Interestingly, among the 80 TFs identified from this microarray analysis, only *AtERF070* (*At1g71130*), belonging to the B5 subfamily of ETHYLENE RESPONSE FACTOR (ERF) TFs, showed early induction during short-term Pi deprivation and also remained induced when the Pi deficiency treatment was extended for a long term (Misson et al., 2005). Although the microarray analysis suggested this TF to be highly responsive to Pi deficiency, it has not yet been functionally characterized.

In this study, we have employed RNA interference (RNAi)-mediated suppression and constitutive overexpression of *AtERF070* to determine the role of this TF in maintaining Pi homeostasis. Although RNAi-mediated suppression of *AtERF070* resulted in a pronounced increase in root growth and Pi content, there was no significant effect on the expression of PSR genes. On the contrary, the overexpression of this gene resulted in a retarded growth phenotype and modulation in the expression of several PSR and GA biosynthetic genes. Thus, this study indicates the role of this TF in maintaining Pi homeostasis and potential cross talk with the phytohormone signaling pathway.

RESULTS

Pi Deficiency-Mediated Differential Spatial Expression of *AtERF070* and Subcellular Localization of Its Fusion Protein

Pi deficiency triggers differential regulation of an array of PSR genes. To obtain a more comprehensive insight into the effects of Pi deprivation on the spatial expression of *AtERF070*, real-time PCR analyses were carried out for both vegetative (roots and shoots) and reproductive (flowers) tissues of the wild-type seedlings grown hydroponically in the greenhouse under P+ (250 μM Pi) and P− (0 μm Pi) conditions for 7 d. Pi deficiency triggered a significant increase in the relative expression of *AtERF070* in both roots and shoots, but its relative expression was comparable in the flowers irrespective of the Pi regime (Fig. 1A). The data not only confirmed earlier microarray analysis (Misson et al., 2005) but also highlighted the differential spatial regulation of this gene, signifying its potential role in the maintenance of Pi homeostasis. To further determine the effect of other nutrient deficiencies on the relative expression of *AtERF070*, wild-type Arabidopsis seedlings were also subjected to potassium, nitrogen, and iron deficiencies for 7 d. None of these nutrient deficiencies illicit any significant induction of this gene in the seedlings (data not shown), thereby demonstrating the specific responsiveness of this gene to Pi deprivation.

Subcellular localization is an important characteristic of TFs, and it plays a critical role in regulating the nutrient starvation responses (Beck and Hall, 1999). Therefore, for ascertaining the subcellular localization of *AtERF070*, its coding region was fused with the 3′ end of an *EGFP* (for enhanced GFP) reporter gene and expressed constitutively under the control of the cauliflower mosaic virus (CaMV) 35S promoter. *EGFP* under the control of the CaMV 35S promoter was used as a control. Stable transgenic Arabidopsis plants expressing reporter *35S*::*EGFP* alone (control) and chimeric *35S*::*EGFP*::*AtERF070* were analyzed for their subcellular localization under P+ and P− conditions (Fig. 1B). The GFP fluorescence was localized to the nucleus in the *35S*:*GFP*::*AtERF070* transgenic lines irrespective of the Pi regime, whereas the distribution of GFP fluorescence was uniform throughout the cell of the control plant. Furthermore, the nuclear localization of GFP::AtERF070 protein was confirmed by staining the nucleus with 4′,6-diamidino-2-phenylindole (DAPI; Fig. 1C). Bioinformatic analysis of the amino acid sequence of AtERF070 showed an ERF domain toward the C-terminal end of the protein (Fig. 1D).

AtERF070 RNAi Lines Show Altered Morphophysiological Traits

RNAi-mediated gene silencing has been successfully used for the functional characterization of different TFs in Arabidopsis (*WRKY75*; Devaiah et al., 2007a) and rice (*Oryza sativa*; *OsPHR1* and *OsPHR2* [Zhou et al., 2008] and *OsMYB2P-1* [Dai et al., 2012]) that play a pivotal role in the maintenance of Pi homeostasis. Therefore, a similar strategy was used to determine the role of *AtERF070*, if any, in the acquisition and/or mobilization of Pi. Two independent RNAi mutant lines (RNAi4 and RNAi11) were used for comprehensive evaluation. Real-time PCR analysis was employed for determining the extent of attenuation in the expression of *AtERF070* in RNAi seedlings grown under P+ and P− conditions on agar petri plates for 7 d (Fig. 2A). Under both P+ and P− conditions, RNAi-mediated silencing triggered about 65% to 70% reductions in the expression of *AtERF070* in RNAi4 and RNAi11 seedlings compared with their respective wild-type seedlings. These two RNAi lines

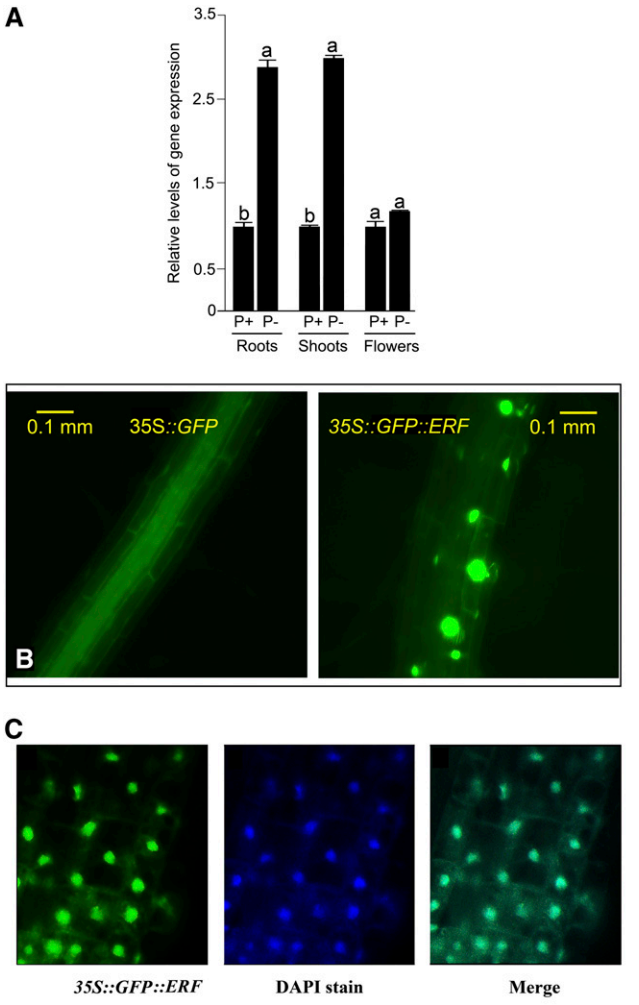

Figure 1. Pi deficiency-induced differential spatial expression of *AtERF070* and subcellular localization of its fusion protein. A, Four-week-old wild-type seedlings were grown hydroponically and then subjected to P+ (250 μM Pi) and P− (0 μM Pi) treatments for 7 d. Real-time PCR analyses of *AtERF070* in different tissues (roots, shoots, and flowers) of hydroponically grown seedlings under P+ and P− conditions was performed. *AtACTIN2* was used as an internal control, and P+ values were normalized to 1. Data presented are means of six technical replicates ± SE. Different letters indicate significant differences in the relative level of gene expression. B, Subcellular localization of a GFP::AtERF070 fusion protein. C, Colocalization of GFP::AtERF070 and the nucleus-specific dye DAPI. Shown from left to right are GFP fluorescence, staining of the nucleus by DAPI, and a merged image. D, Amino acid sequence of AtERF070 with the shaded region depicting the ERF domain. The β-sheet and α-helix are depicted in red and blue, respectively, in the shaded region of the sequence. Letters in yellow and cyan represent the two conserved domains CMVI-1 and CMVI-2, respectively, while the letters in pink indicate an overlapping region between them. [See online article for color version of this figure.]

were subsequently used for detailed morphophysiological characterization (Fig. 2, B–G). Under both P+ and P− conditions, there were significant ($P \leq 0.05$) increases in total Pi content of roots and shoots, and total shoot area, of both the RNAi lines compared with their respective wild-type controls (Fig. 2, B and C). Since RNAi4 and RNAi11 exhibited elevated Pi content and shoot area, it was assumed that these morphophysiological changes could possibly be due to modulation of the root system that plays a pivotal role in Pi acquisition and mobilization (Williamson et al., 2001; López-Bucio et al., 2002, 2005; Jain et al., 2007b, 2009; Lynch, 2011). Also, mutations in the Pi-responsive TFs *WRKY75* and *PRD* have been shown to affect different root traits under different Pi regimes (Devaiah et al., 2007a; Camacho-Cristóbal et al., 2008; Jain et al., 2012). Therefore, different traits of the RSA of *AtERF070* RNAi lines grown under P+ and P− conditions for 7 d on agar petri plates were compared with their respective wild types (Fig. 2, D–G). There was a noticeable exaggerated root growth of both P+ and P− RNAi4 and RNAi11 lines compared with their respective wild-type seedlings (Fig. 2D) due to significant ($P \leq 0.05$) increases in both primary root growth (Fig. 2E) and the number and length (Fig. 2, F and G) of first- and higher-order lateral roots. Mutant analyses of some of the TFs (*PHR1*, *WRKY75*, and *BHLH32*) demonstrated their differential regulatory influence on root hair development under different Pi regimes (Chen et al., 2007; Devaiah et al., 2007a; Bustos et al., 2010). Therefore, we compared the developmental responses of root hairs in RNAi4 and RNAi11 lines with the wild type during growth under P+ and P− conditions (Fig. 3). Under both P+ and P− conditions, there was a significant ($P \leq 0.05$) increase in the number of root hairs in the 5-mm region of the primary root tip of RNAi4 and RNAi11 compared with their corresponding wild types (Fig. 3).

Overexpression of *AtERF070* Attenuates Pi Content and Different Traits of RSA

Overexpression lines, harboring the full-length complementary DNA (cDNA) of *AtERF070* under the control of a CaMV 35S promoter, were generated (hereafter referred to as Oe1 and Oe2) and evaluated for changes in Pi content and different traits of RSA under P+ and P− conditions (Fig. 4). Two independently generated overexpressors revealed 40- to 60-fold increases in the relative expression of *AtERF070* in 12-d-old seedlings grown under nutrient-rich conditions compared with the wild type (Fig. 4A). These overexpressors were subsequently used for morphophysiological characterization. Under both P+ and P− conditions, the overexpression lines (Oe1 and Oe2) showed significant ($P \leq 0.05$) reductions in Pi contents in both roots and shoots (Fig. 4B). The overexpression lines germinated on one-half-strength Murashige and Skoog (MS) medium showed a distinct accumulation of anthocyanin that intensified on day 4 post germination (Fig. 4C, top), which

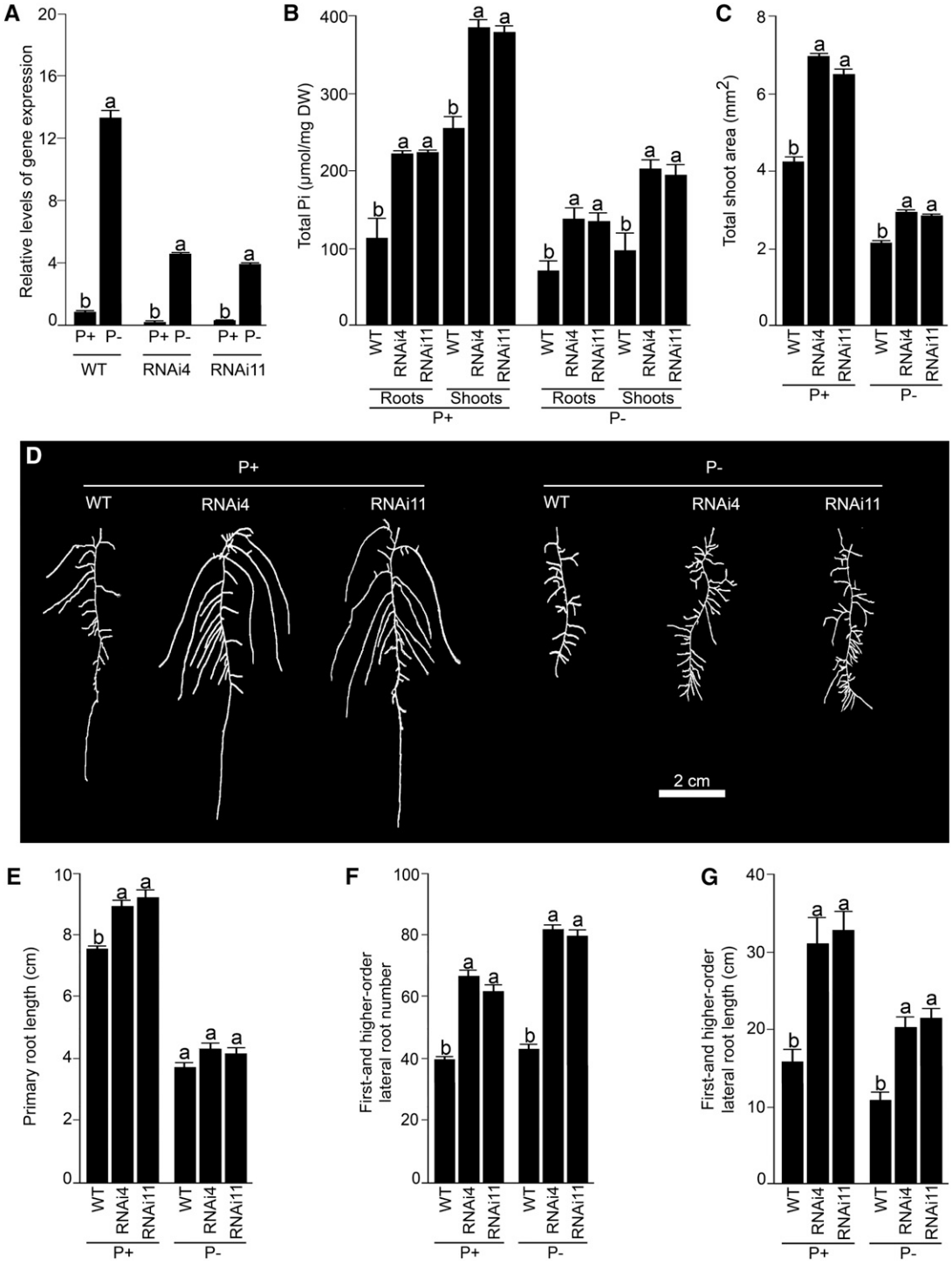

Figure 2. RNAi-mediated silencing of *AtERF070* modulates morphophysiological traits. Arabidopsis (wild-type [WT] and RNAi lines) seedlings were raised initially on vertically oriented agar petri plates containing one-half-strength MS for 5 d and then transferred to P+ and P− media for 7 d. A, The whole seedling was used for real-time PCR analyses of *AtERF070* as described in the legend to Figure 1. The wild-type P+ value was normalized to 1. Different letters indicate significant differences in the relative level of gene expression. B to G, Roots and shoots of the wild-type and *AtERF070* RNAi lines were separated at the hypocotyl-root junction. Data are presented for total Pi content (B), total shoot area (C), root architectural details (D), primary root length (E), first- and higher-order lateral root number (F), and their length (G). Values are means ± SE, and $n = 6$ replicates of 10 seedlings each (B) or $n = 10$ (C and E–G). Different letters on the histograms indicate that the means differ significantly ($P \leq 0.05$). DW, Dry weight.

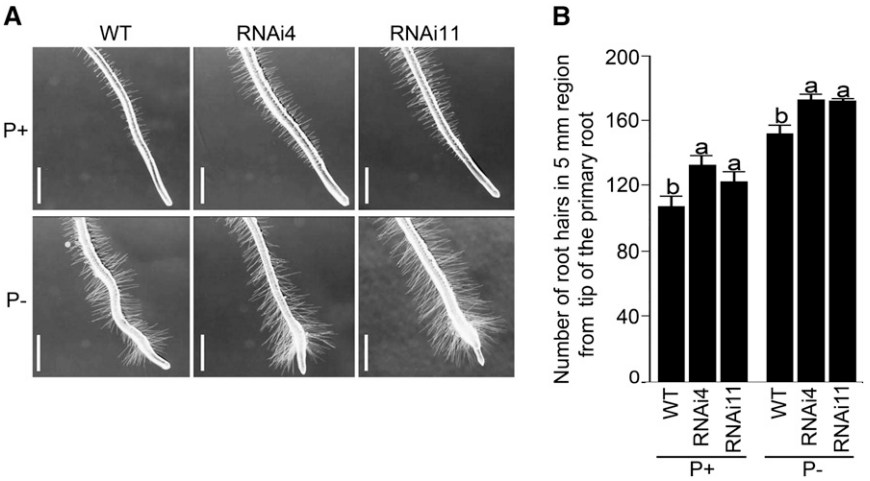

Figure 3. Root hair development is enhanced in *AtERF070* RNAi lines. Arabidopsis (wild-type [WT] and RNAi lines) seedlings were raised as described in the legend to Figure 2 under P+ and P− conditions for 2 d. A, Development of root hairs in a 5-mm region of the primary root tip of wild-type and RNAi seedlings grown under P+ and P− conditions. Bars = 1 mm. B, Total number of root hairs in a 5-mm region of the primary root tip. Values are means ± SE; $n = 10$. Different letters on the histograms indicate that the means differ significantly ($P \leq 0.05$).

was 6-fold higher compared with the wild-type seedlings (Fig. 4C, bottom). Also, under P+ and P− conditions, there were significant ($P \leq 0.05$) increases in root-shoot ratio of both the overexpression lines compared with the wild type (Fig. 4D). Furthermore, the RSA of overexpression lines grown on P+ and P− media on vertically oriented agar plates for 7 d was documented (Fig. 4E). Irrespective of Pi regime, both the overexpression lines overall displayed a relatively smaller root system compared with the wild type. The effect of overexpression on the growth of primary root was more pronounced in Oe1 under both P+ and P− conditions (Fig. 4F). Interestingly though, the inhibitory effects of *AtERF070* overexpression were evident on both the number and the length of first- and higher-order lateral roots of Oe1 and Oe2 (Fig. 4, G and H). Relatively, the effect of the overexpression of *AtERF070* was more pronounced on lateral root development than on primary root growth. The differential effect of *AtERF070* on the primary and lateral roots could be attributed to their distinct ontogeny. These results thus suggested a potential role of *AtERF070* in regulating the growth and development of RSA that, in turn, affects Pi homeostasis.

AtERF070 Overexpression Lines Display Retarded Growth Responses

Wild-type, *AtERF070* RNAi, and overexpression lines were germinated and grown to maturity on a Premier ProMix PGX peat mix under greenhouse condition for documenting different morphometric traits (Fig. 5). The overexpression lines exhibited retarded growth until 45 d after germination, resulting in a smaller rosette diameter compared with wild-type and RNAi lines (Fig. 5). Subsequently, overexpression lines developed a large number (around 60) of rosette leaves, resulting in a dwarf bushy appearance (Fig. 5, C–E). Furthermore, the bolting was delayed by 2 weeks in both the overexpression lines compared with the wild-type and RNAi lines (Fig. 5F). Interestingly, overexpression lines also produced around 20 to 24 inflorescence branches, which were about 3-fold higher than that produced by either wild-type or RNAi lines (Fig. 5G). The overexpression lines exhibited a delay in the onset of senescence and eventually completed their life cycle 2 weeks later than the wild-type and RNAi lines (data not shown).

GA Supplementation-Mediated Partial Recovery of the Growth Responses of the Overexpression Lines

Since *AtERF070* overexpression lines displayed a phenotype similar to GA-deficient mutant (Fu and Harberd., 2003) and *MYB62* overexpression (Devaiah et al., 2009) lines, we presumed that the *AtERF070* overexpression phenotype could possibly be rescued by supplementing the growth medium with GA. Therefore, wild-type and overexpression lines were grown under Pi-replete condition supplemented with and without GA_3 (1 μM) on vertically oriented petri plates for 7 d (Fig. 6). The primary root length and number of first- and higher-order lateral roots of the wild-type seedlings were comparable during growth on P+ and GA_3-supplemented P+ medium (Fig. 6, A–C). On the contrary, there was a significant ($P \leq 0.05$) increase in both the length of the primary root and the number of first- and higher-order lateral roots of the overexpression lines when grown on GA_3-supplemented P+ medium (Fig. 6, A–C), whereas the effect of GA_3 supplementation in P+ medium on the augmented growth of the first- and higher-order lateral roots was relatively comparable in wild-type and overexpression lines (Fig. 6D). Although GA_3 supplementation in the P+ medium triggered an increase in the growth responses of different root traits in overexpression lines, the root phenotype was still not comparable to that of the wild-type seedling grown on P+ medium. This suggested a rather partial recovery of the root phenotype of overexpression lines by GA_3 treatment. Furthermore, the role of GA in recovering the phenotype of the aerial parts of the overexpression lines grown under greenhouse conditions was tested. The overexpression lines and the wild type were grown on Premier ProMix PGX peat mix for 2 weeks and

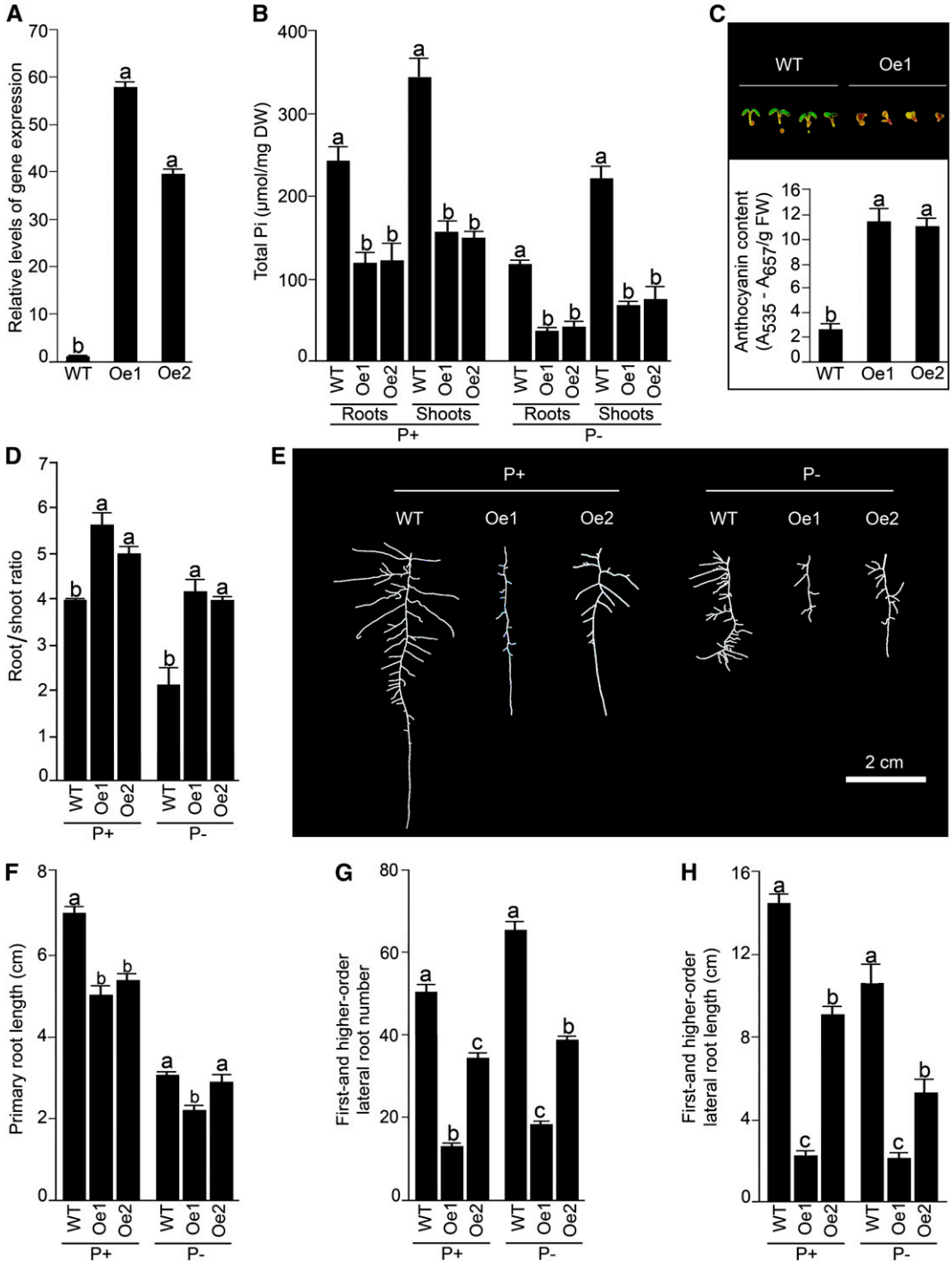

Figure 4. Overexpression of *AtERF070* affects morphophysiological responses. Arabidopsis (wild-type [WT] and Oe1 and Oe2) seedlings were raised as described in the legend to Figure 2. A, Whole seedlings (the wild type and Oe1 and Oe2) raised on one-half-strength MS medium were used for real-time PCR analyses of *AtERF070* as described in the legend to Figure 1. The wild-type P+ value was normalized to 1. Different letters indicate significant differences in the relative level of gene expression. B to H, Roots and shoots of the wild type and Oe1 and Oe2 were dissected at the hypocotyl-root junction. Data are presented for total Pi contents in roots and shoots; $n = 6$ replicates of 25 seedlings each (B), accumulation (top) and quantification (bottom) of anthocyanin content in the shoots; $n = 6$ replicates of 100 seedlings each (C), root-shoot ratio; $n = 6$ replicates of 25 seedlings each (D), root architectural details (E), primary root length (F), first- and higher-order lateral root number (G), and their length (H); $n = 10$ for F to H. Values are means ± SE, and different letters on the histograms indicate that the means differ significantly ($P \leq 0.05$). DW, Dry weight; FW, fresh weight. [See online article for color version of this figure.]

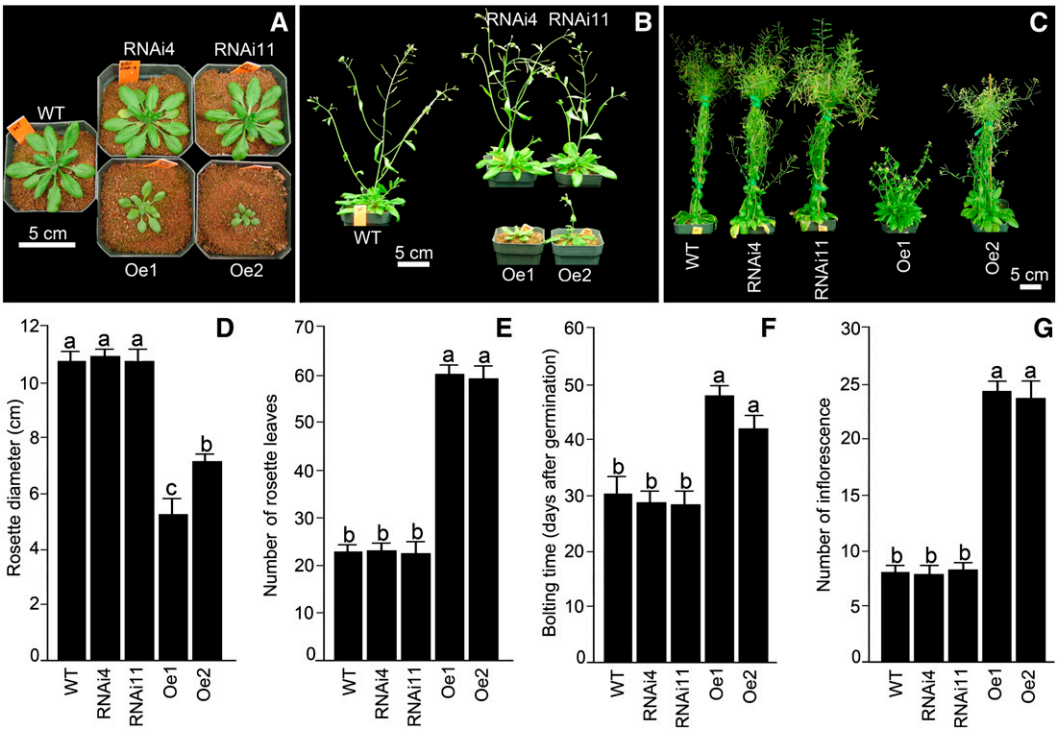

Figure 5. Differential temporal growth responses of *AtERF070* RNAi and overexpression lines. A to C, Wild-type (WT), *AtERF070* RNAi, and overexpression lines were germinated in potting mix and grown under greenhouse conditions, and their temporal growth responses were documented 30 d (A), 45 d (B), and 70 d (C) after germination. D to G, Data are presented for rosette diameter (D), number of rosette leaves (E), bolting time (F), and number of inflorescences (G). Values are means ± SE, and $n = 10$. Different letters on the histograms indicate that the means differ significantly ($P \leq 0.05$). [See online article for color version of this figure.]

sprayed eight times on alternate days with GA_3 (100 μM) or GA_4 (50 μM). As a control, both overexpression lines and wild-type plants were sprayed with water for the same duration. The apical dominance and time of bolting in both overexpression lines could be restored by spraying with GA_3 or GA_4 (Fig. 7A). In addition, spraying with either GA_3 or GA_4 partially recovered the phenotype of lateral branches, length of primary inflorescence, and rosette diameter of the overexpression lines (Fig. 7, B and C). However, spraying with either GA_3 or GA_4 did not have any effect on the number of rosette leaves produced by overexpression lines, which remained significantly ($P \leq 0.05$) higher than those of the wild type (data not shown).

Overexpression of *AtERF070* Alters the Expression of a Subset of PSR and GA Biosynthetic Genes

To determine the relative expression of some of the functionally characterized PSR genes (i.e. *HIGH-AFFINITY PHOSPHATE TRANSPORTER1;1* [*Pht1;1*], *Pht1;4*, *INDUCED BY PHOSPHATE STARVATION1* [*IPS1*], *ACID PHOSPHATASE5* [*ACP5*], *RIBONUCLEASE1* [*RNS1*], *At4*, *microRNA399b*, and *microRNA399f*; Muchhal et al., 1996; Bariola et al., 1999; del Pozo et al., 1999; Martín et al., 2000; Karthikeyan et al., 2002; Shin et al., 2004, 2006; Fujii et al., 2005) in the seedlings by real-time PCR, the wild-type, RNAi, and overexpression lines were grown under P+ and P− conditions for 7 d in vertically oriented agar plates. The relative expression levels of these PSR genes were comparable in both wild-type and RNAi seedlings under both P+ and P− conditions (Fig. 8), whereas there was a significant increase in the expression of *RNS1* in overexpression seedlings compared with wild-type seedlings. On the contrary, the relative expression of *At4* was suppressed in both P+ and P− overexpression seedlings compared with wild-type seedlings. There was an increase in the relative expression of *microRNA399b*, *microRNA399f*, and *ACP5* only in P− overexpression seedlings compared with wild-type seedlings. However, the relative expression of *AtIPS1*, *Pht1;1*, and *Pht1;4* in overexpression lines was comparable irrespective of Pi regime. These results clearly suggested differential effects of overexpressing *AtERF070* on a subset of PSR genes. Since the root and shoot phenotypes of overexpression lines could be recovered partially by exogenous GA application (Figs. 6 and 7), this suggested a likely effect of overexpressing *AtERF070* on the relative expression of some of the genes involved in GA biosynthesis. Interestingly, the relative expression levels of *Arabidopsis thaliana ent-Kaurene synthase* (*AtKS*), mediating the first committed step in GA biosynthesis, along with *Arabidopsis thaliana ent-Kaurenoic acid oxidase1* and *Arabidopsis thaliana GA2oxidase2* (*AtGa2ox2*) were down-regulated in overexpression lines under both P+ and P− conditions. Although the relative expression of *AtGa3ox2* was

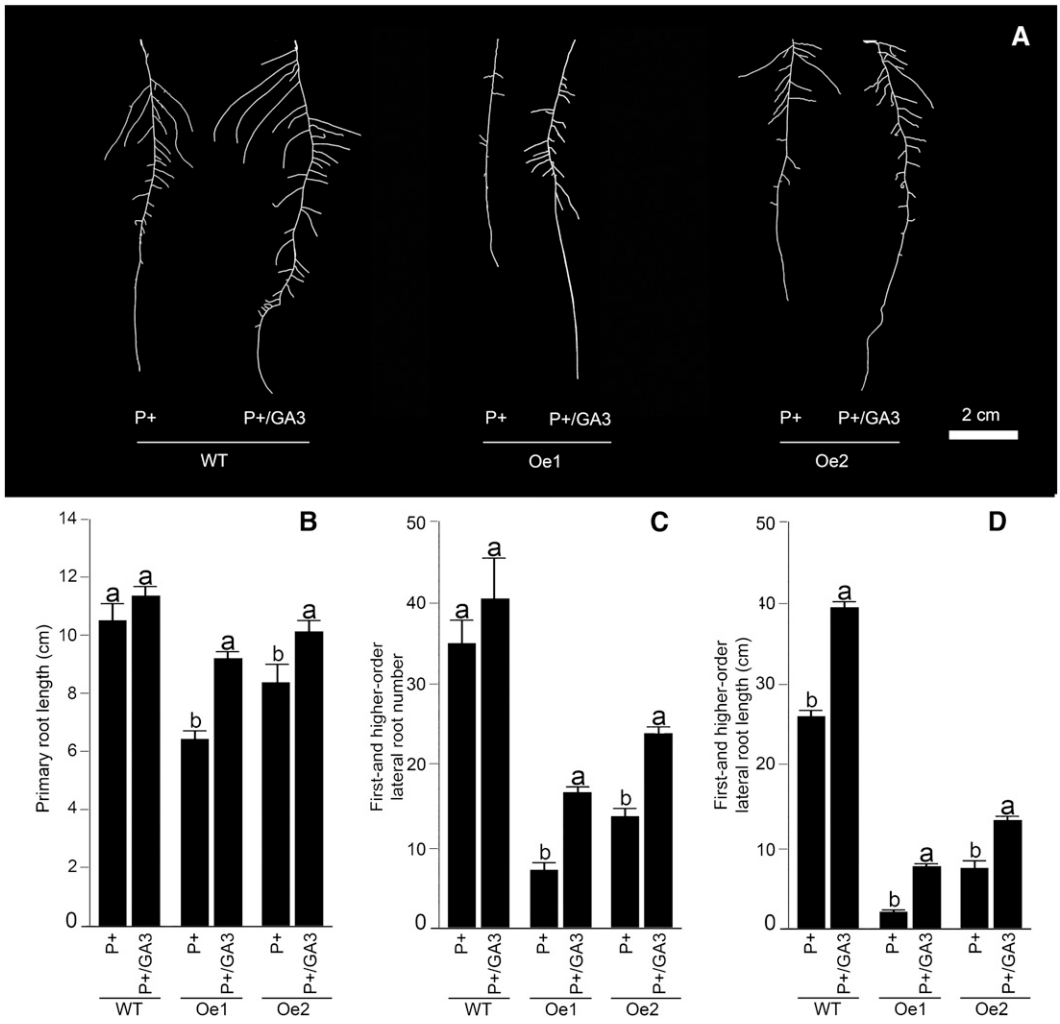

Figure 6. Growth medium supplemented with GA modulates the RSA of *AtERF070* overexpression lines. A, Wild-type (WT) and *AtERF070* overexpression lines were germinated on one-half-strength MS medium for 7 d and then transferred to P+ medium with or without 1 μM GA_3. Lateral roots were spread to reveal details of RSA and are representative of 10 seedlings each for the wild-type and overexpression lines. B to D, Data are presented for the effects of GA treatment on primary root length (B), first- and higher-order lateral root number (C), and first- and higher-order lateral root length (D) of wild type and transgenics. Values are means ± SE, and $n = 10$. Different letters on the histograms indicate that the means differ significantly ($P \leq 0.05$).

down-regulated in P+ overexpression lines, there was a significant increase in the relative expression of this gene in P− overexpression lines. However, the relative expression levels of several other genes that are involved in the GA biosynthetic pathway (*AtKO*, *AtGa3ox1*, *AtGa2ox1*, *AtGa20oxs*) were comparable in overexpression and wild-type seedlings under both P+ and P− conditions. These results further suggest the effect of overexpressing *AtERF070* on a subset of genes that are involved in the GA biosynthetic pathway (Fig. 9).

DISCUSSION

TFs regulate a diverse group of genes during stress responses and are important components of gene regulatory networks (Yamaguchi-Shinozaki and Shinozaki, 2006). TFs also play an important role in the maintenance of Pi homeostasis (Jain et al., 2012). In Arabidopsis, the AP2/ERF TF superfamily comprises 147 members, including the AP2 and ERF families (Riechmann et al., 2000; Feng et al., 2005). AP2/ERF proteins are known to regulate the responses of plants to various biotic and abiotic stresses and developmental processes (Elliott et al., 1996; Stockinger et al., 1997; Gu et al., 2000; Boutilier et al., 2002; Dubouzet et al., 2003). In this study, we report the functional characterization of *AtERF070*, a member of the AP2/ERF family.

AtERF070 Is a PSR Nucleus-Localized TF

The expression of *AtERF070* is induced significantly and specifically in Pi-starved roots and leaves (Fig. 1A), and the results were consistent with an earlier study (Misson et al., 2005). Several other functionally characterized TFs (i.e. *WRKY6-1*, *WRKY75*, *ZAT6*, *MYB62*, *PRD*,

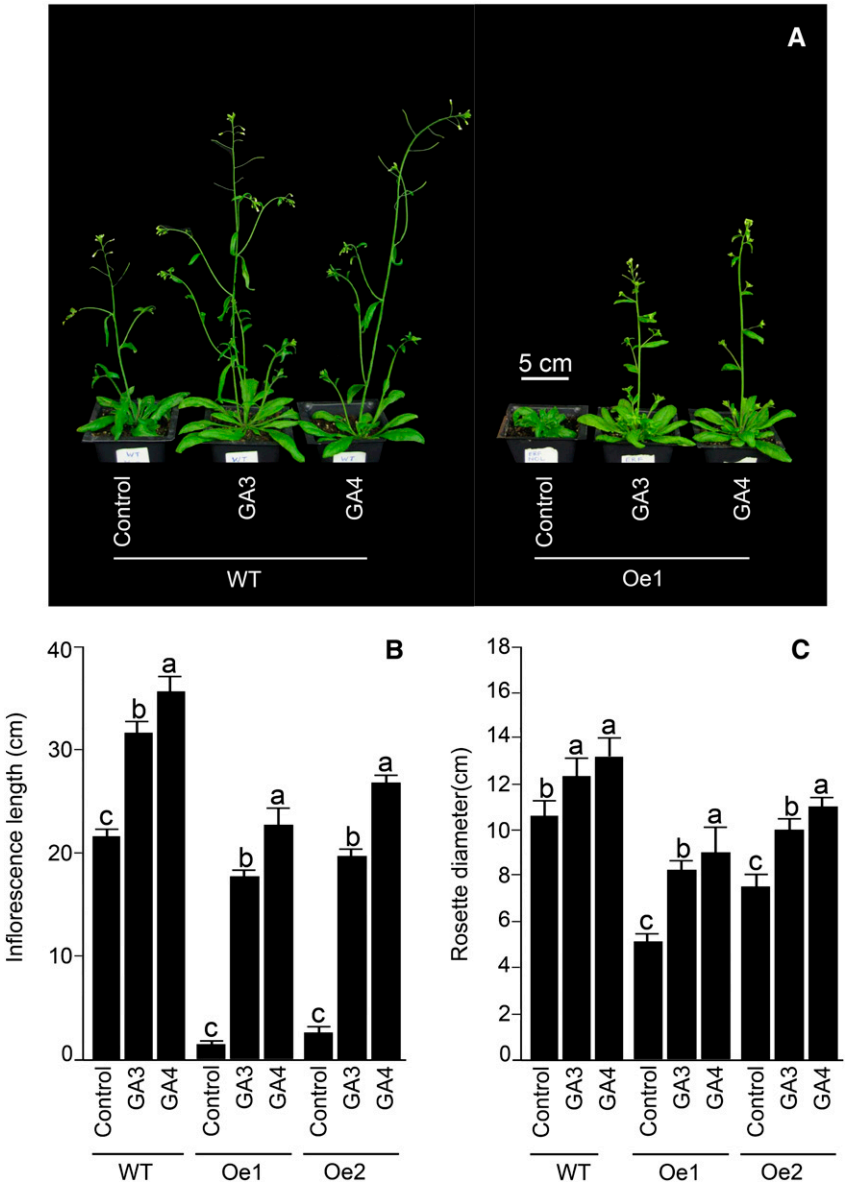

Figure 7. Exogenous GA application partially restores the shoot phenotype of *AtERF070* overexpression lines. A, Effects of GA application on wild-type (WT) and *AtERF070* overexpression lines. Wild-type and *AtERF070* overexpression lines were germinated on soil, and 20-d-old plants were treated with 50 μM GA_4 or 100 μM GA_3 on alternate days. A total of eight sprays were carried out, and control plants were treated with water. B and C, Data are presented for the effects of exogenous GA application on inflorescence length (B) and rosette diameter (C) of wild type and transgenics. Values are means ± SE (n = 10). Different letters on the histograms indicate that the means differ significantly ($P \leq 0.05$). [See online article for color version of this figure.]

HRS1-1, *bHLH32*, *BnPHR1 OsPTF1*, and *OsMYB2P-1*) have been shown to be differentially regulated under different Pi regimes and to play a role in the maintenance of Pi homeostasis (Yi et al., 2005; Chen et al., 2007; Devaiah et al., 2007a, 2007b, 2009; Camacho-Cristóbal et al., 2008; Liu et al., 2009; Dai et al., 2012; Ren et al., 2012). Although *PHR1*, *OsPHR1*, and *OsPHR2* are not responsive to Pi deficiency, they have also been implicated in regulating a subset of PSR genes (Rubio et al., 2001; Bari et al., 2006; Zhou et al., 2008; Bustos et al., 2010).

The localization of TFs could play a major role in determining their function. For example, the target of Rapamycin signaling pathway is implicated in the cytoplasmic retention of several TFs, thereby preventing the transcription of downstream genes induced by nitrogen limitation (Beck and Hall, 1999). In the yeast (*Saccharomyces cerevisiae*) phosphatase (PHO) regulon, Pi-starvation-induced nuclear localization of Pho4 has been shown to be a prerequisite for its activity in transcriptional regulation (Ogawa et al., 1995; Lenburg and O'Shea, 1996). Interestingly, *AtERF070* is localized to the nucleus irrespective of Pi regime. This pattern of Pi-independent localization is also a characteristic feature of some of the Pi-starvation-induced TFs in Arabidopsis (*WRKY75*, Devaiah et al., 2007a; *ZAT6*, Devaiah et al., 2007b; *MYB62*, Devaiah et al., 2009) and rice (*OsPTF1*, Yi et al., 2005). Regulation of these TFs by posttranslational modifications, protein-protein interaction, DNA-protein interaction, and/or chromatin modifications has been postulated (Schwechheimer and Bevan, 1998; Miura et al., 2005).

AtERF070 RNAi Lines Have Higher Pi Accumulation and Increased Root Growth

To decipher the in planta role of *AtERF070* in regulating Pi homoeostasis, two independent RNAi lines

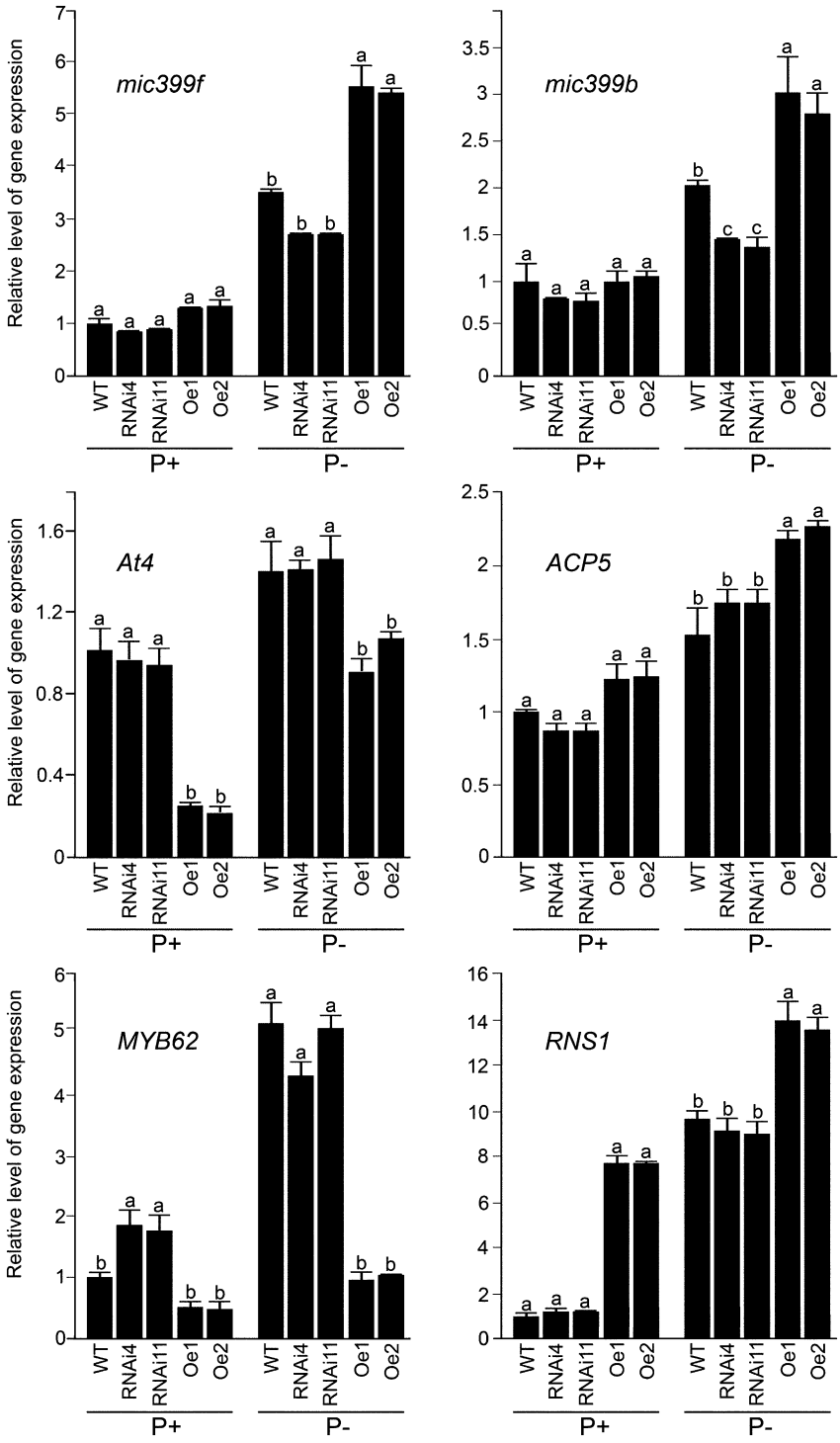

Figure 8. Real-time PCR analysis of PSR genes in *AtERF070* RNAi and overexpression lines. Wild-type (WT), RNAi, and overexpression seedlings were germinated on one-half-strength MS medium for 7 d and then transferred to vertically oriented agar petri plates containing P+ and P− media for 1 week. Whole seedlings were harvested and used for real-time PCR analysis revealing the relative expression levels of PSR genes in the wild type and transgenics. The Arabidopsis housekeeping gene *AtACTIN2* (*At3g18780*) was used as an internal control. Expression values for the PSR genes in wild-type P+ were set at 1. The values presented are means of three technical replicates ± SE. Different letters indicate significant differences.

were analyzed. As anticipated, there was a significant decrease in the expression of *AtERF070* in both RNAi lines. The *AtERF070* RNAi lines displayed increases in Pi content and shoot area irrespective of Pi regime. A similar increase in Pi content was also observed in the *WRKY75RNAi* lines under both P+ and P− conditions (Devaiah et al., 2007a), whereas *wrky6-1* showed an increased accumulation of Pi only in P+ shoots (Chen et al., 2009). In contrast, the Pi contents of *prd*, *hrs1-1*, *Osphr1RNAi*, and *Osphr2RNAi* lines were comparable to their respective wild types irrespective of the Pi regime. On the contrary, *phr1* showed a significant reduction in the Pi content of the P+ seedlings compared with the wild type (Rubio et al., 2001; Bustos et al., 2010). Therefore, higher Pi accumulation as a result of the reduced expression of *AtERF070* in the RNAi lines suggests that it is a negative regulator of Pi homeostasis.

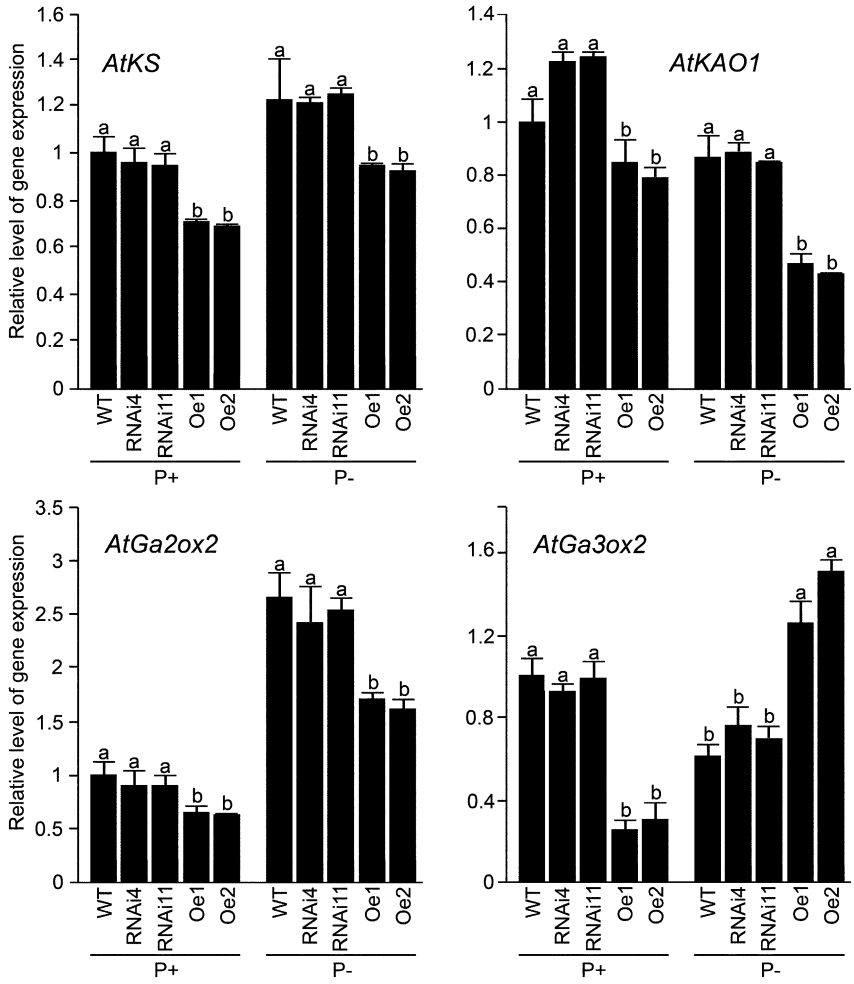

Figure 9. Real-time PCR analysis of GA biosynthetic genes in *AtERF070* RNAi and overexpression lines. Wild-type (WT), RNAi, and overexpression seedlings were germinated on one-half-strength MS medium for 7 d and then transferred to vertically oriented agar petri plates containing P+ and P− media for 1 week. Whole seedlings were harvested and used for real-time PCR analysis revealing the relative expression levels of GA biosynthetic genes in the wild type and transgenics. The Arabidopsis housekeeping gene *AtACTIN2* (*At3g18780*) was used as an internal control. Expression values for the GA biosynthetic genes in wild-type P+ were normalized to 1. Different letters indicate significant differences in the relative level of gene expression. The values presented are means of three technical replicates ± SE.

RSA is a critical component of plant adaptation to the heterogenous distribution of Pi in soils. RSA comprises ontogenetically distinct embryonic and postembryonically developed primary and lateral roots, respectively. Primary root growth was augmented in the *AtERF070* RNAi lines under Pi-sufficient conditions, suggesting that it is a negative regulator of this root trait. This is in contrast to an inhibitory effect on the primary root growth in P− *prd* seedlings (Camacho-Cristóbal et al., 2008), which suggested a positive regulatory effect of *PRD* on Pi-deficiency-mediated primary root growth. Relatively, there were no noticeable variations in primary root growth of *OsPHR2RNAi*, *WRKY75RNAi*, *bhlh32*, and *hrs1-1* compared with their respective wild type (Zhou et al., 1997; Chen et al., 2007; Devaiah et al., 2007a; Liu et al., 2009). In addition, *AtERF070* RNAi lines also showed a significant increase in root hair number (Fig. 3). Similar increases in root hair numbers have also been reported for *bhlh32* and *WRKY75* RNAi lines (Chen et al., 2007; Devaiah et al., 2007a). These results indicate that *AtERF070*, in coordination with other TFs, regulates root hair development. An earlier report implicated ethylene in both root hair initiation and elongation (Dolan, 2001). Under nutrient deficiency, including Pi starvation, auxin and ethylene are known to play major roles in root hair development (Masucci and Schiefelbein, 1994). Our results show that an ERF that is the downstream target of the ethylene signaling pathway is involved in root hair development.

In addition, the *AtERF070* RNAi lines displayed significant increases in the number and length of the lateral roots, which was similar to the augmented lateral root growth of the *WRKY75RNAi* lines (Devaiah et al., 2007a). Interestingly, the PSR TFs *ZAT6*, *MYB62*, *PRD* (Devaiah et al., 2007b, 2009; Camacho-Cristóba et al., 2008), and *AtERF070* modulate the growth of both primary and lateral roots, while *WRKY75* regulates the growth of lateral roots only (Devaiah et al., 2007a). These results suggest that different TFs have differential effects on the developmental responses of the root system.

Overexpression of *AtERF070* Displays Stunted Root Growth

Overexpression of *AtERF070* resulted in reductions of primary root length, lateral root number, and lateral root length irrespective of Pi regime (Fig. 4). This decrease in the primary root growth was similar to the stunted primary root exhibited by *ZAT6* and *MYB62* overexpression lines (Devaiah et al., 2007b, 2009). While

the *ZAT6* overexpressors compensated this by augmenting the lateral root growth, the *AtERF070* and *MYB62* overexpression lines (Devaiah et al., 2009) displayed a decreased lateral root growth relative to their respective wild types. Interestingly, *ZAT6* and *MYB62* overexpression lines also showed altered root parameters under both P+ and P− conditions (Devaiah et al., 2007b, 2009).

In the case of the *AtERF070* overexpression lines, the reduced root growth could have led to the lower Pi content relative to the wild type (Fig. 4B). Comparatively, the *ZAT6* overexpression lines exhibited decreased Pi content (Devaiah et al., 2007b), while the *MYB62* overexpressors had a higher Pi content in P+ shoots and a lower Pi content in the P− seedlings, relative to the wild type (Devaiah et al., 2009). The decrease in the Pi content of the *AtERF070* overexpression lines could have triggered higher anthocyanin accumulation (Fig. 4C), which is similar to that observed in the *ZAT6* and *MYB62* overexpressors (Devaiah et al., 2007b, 2009). Taken together, these studies suggest that different TFs induced during Pi deficiency coordinately regulate multiple Pi-starvation responses.

Overexpression of *AtERF070* Modulates Plant Growth

Overexpression of *AtERF070* resulted in stunted plants lacking apical dominance with delayed bolting and senescence, which are reminiscent of a GA-deficient plant (Fig. 5). Interestingly, the *AtERF070* overexpression lines had a phenotype similar to the *MYB62* overexpression line (Devaiah et al., 2009), suggesting that both TFs may be involved in the cross talk between GA and Pi starvation. This assumption was confirmed by treating *AtERF070* overexpression lines with GA.

GA_3-treated 7-d-old seedlings of *AtERF070* overexpression lines showed increased primary root growth, higher lateral root number, modest increase in lateral root length, and restoration of apical dominance, pointing toward a partial recovery of the phenotype. This response is similar to the recovery of *ga1-3*, a GA-deficient mutant, by an exogenous supplementation of GA (Fu and Harberd, 2003). Partial reversal of the phenotype by GA application further substantiated the reasoning that the overexpression lines are GA deficient. To further confirm this, we analyzed the relative expression of GA biosynthetic genes in the *AtERF070* overexpression and RNAi lines relative to the wild-type plants. In Arabidopsis, *AtKS*, *Arabidopsis thaliana ent-Kaurenoic acid oxidase1*, and *AtGA2oxs* are implicated in the GA biosynthetic pathway. Overexpression of *AtERF070* resulted in significant attenuation in the relative expression of these genes. Even a marginal attenuation in the expression of *AtKS* could have an impact on GA content, since it is encoded by a single gene and is involved in the first committed step in GA biosynthesis (Olszewski et al., 2002). This suggested that the *AtERF070* overexpression lines had altered expression of a subset of GA biosynthetic genes, which could possibly result in reduced GA in these lines. Interestingly, the subset of GA biosynthetic genes attenuated in the *MYB62* overexpression lines was different (Devaiah et al., 2009) from those altered in *AtERF070* overexpression lines. Although these two TFs affect different aspects of the GA biosynthetic pathway, they both seem to modulate GA levels, causing a similar plant phenotype in their overexpression lines. An earlier study demonstrated a reduction in bioactive GA levels during Pi starvation (Jiang et al., 2007). A number of the Pi-deficiency-mediated morphological changes are associated with a lack of GA (O'Rourke et al., 2013). Therefore, potential roles of *AtERF070* and *MYB62* in mediating a cross talk between phytohormone and Pi-sensing and -signaling cascades could be assumed.

PSR Genes Are Modulated in *AtERF070* Overexpression Lines

Among the PSR genes, *microRNA399f* and *microRNA399b* were up-regulated in the Pi-deprived *AtERF070* overexpression lines. However, an elevated relative expression of *microRNA399b* in the *AtERF070* overexpression lines neither altered *Pho2* level nor increased Pi content as reported in an earlier study (Lin et al., 2008). A similar increase in the expression of *microRNA399f* was reported in response to an increased expression of the transcriptional activator *AtMYB2* (Baek et al., 2013). In contrast, the *AtERF070* RNAi lines showed a modest suppression of *microRNA399b* only under Pi-deficient conditions. The up-regulation of microRNAs in the *AtERF070* overexpression lines draws focus to the fact that both TFs and microRNAs share their role as regulatory elements. Both of them are trans-acting and bind to cis-elements present in DNA/RNA. In addition, they can regulate a single gene or a number of genes. The point of interest is that they can act together in a specific cell type and establish a particular gene expression pattern in that cell (Hobert, 2004, 2008). This would be of great relevance in Pi starvation, where spatiotemporal regulation of gene expression is a well-established phenomenon. Determining whether *AtERF070* and *microRNA399* work together or in a hierarchical manner could help in understanding regulatory relationships during Pi starvation.

Furthermore, relative expression levels of *Pht1:1*; *Pht1:4*, and *AtIPS1* remained unaltered in the *AtERF070* transgenic lines. This is in contrast to the modulated expression levels of all these genes in the *MYB62* and *ZAT6* overexpression lines (Devaiah et al., 2007b, 2009). Interestingly, *MYB62* is suppressed in the *AtERF070* overexpression lines. This points to the fact that although they might be acting in the same Pi-starvation signaling pathway, they have different and nonoverlapping downstream targets. On the other hand, *At4* was suppressed in the *AtERF070* and *ZAT6* overexpression lines (Devaiah et al., 2007b), although the expression of *ZAT6* remained unaltered in the *AtERF070* overexpression lines. This is indicative of complex interactive pathways of TFs during Pi starvation. A similar

sequential gene regulation has been reported in rice, where the overexpression of *Iron Deficiency-Responsive cis-Acting Element Binding Factor1* caused an increase in the expression of *IRON-RELATED TRANSCRIPTION FACTOR2*, both being TFs involved in iron deficiency responses (Kobayashi et al., 2007).

MATERIALS AND METHODS

Plant Materials and Growth Conditions

Arabidopsis (*Arabidopsis thaliana*) ecotype Columbia was used for generation of the transgenic lines and other experimentation in this study. Wild-type and transgenic seeds were surface sterilized and stratified at 4°C for 2 d. Seeds (20–30) were germinated per petri plate (150 mm × 15 mm) containing one-half-strength MS medium supplemented with 1.5% (w/v) Suc and 1.2% (w/v) agar (Sigma A1296, lot no. 110K0195 with an impurity of 15 μM Pi in 1.2% [w/v] agar [Jain et al., 2009]). The tissue culture and greenhouse growth conditions used were as described (Ramaiah et al., 2011).

Plant Transformation

Arabidopsis plants were transformed by the floral dip method (Clough and Bent, 1998) to generate stable transgenic lines. *AtERF070* RNAi, overexpression, and GFP fusion constructs were used for generating the transgenic lines, and in each case, an empty vector was used for transformation for generating control plants.

The binary vector pGSA1131 was utilized to generate the RNAi construct for *AtERF070*. A 250-bp fragment, unique to the *AtERF070* coding sequence, was amplified using the primers 5′-TCTAGACCATGGTAAAGAGATCGTAAT-3′ and 5′-CCTAGGGGCGCGCCATAAGCTAGAGC-3′. The PCR-amplified fragment was digested with *Nco*I and *Asc*I to facilitate the cloning of the fragment in the sense orientation in the binary vector. The same fragment was then digested with *Xba*I and *Avr*II and cloned in the antisense orientation in the binary vector next to a GUS intron spacer separating the two multiple cloning sites. The presence of the two inserts in the desired orientation was confirmed by sequencing.

The binary vector pEGAD with EGFP as an N-terminal translational fusion was used to generate the GFP::AtERF070 construct. Full-length cDNA of *AtERF070* was amplified using the primers 5′-CCCGGGATGAAGCGTAT-TATCAGAAT-3′ and 5′-AAGCTTTCACGAGCCTCTAGCA-3′. The amplified fragment was cloned in frame with the EGFP after digestion with *Sma*I and *Hin*dIII to generate an N-terminal fusion.

A modified pEGAD vector (Devaiah et al., 2009) was used to generate the overexpression construct for *AtERF070*. Full-length cDNA of *AtERF070* was amplified with the primers 5′-CCCGGGATGAAGCGTATTATCAGAA-3′ and 5′-AAGCTTTCACGCGCCTCTAGCA-3′. The full-length cDNA fragment so amplified was digested with *Sma*I and *Hin*dIII enzymes and cloned next to the CaMV 35S promoter to generate the overexpression construct.

The binary vectors pGSA1131 and pEGAD confer Basta resistance, and the transformed seedlings were recovered by spraying with 50 μL L^{-1} Basta.

GA Treatment

The stocks for GA_4 and GA_3 (Sigma-Aldrich) were prepared by dissolving in alcohol, and the required dilutions were made with water. For greenhouse experiments, GA was sprayed on the aerial parts of the plant. For in vitro experiments, filter-sterilized GA_3 was added to Pi-sufficient medium after autoclaving, and plates were prepared. The spray routine was based on an earlier study involving the rescue of *MYB62*-overexpressing plants by GA application (Devaiah et al., 2009).

Documentation of GFP Fluorescence

A Nikon E800 compound microscope (Diagnostic Instruments) was used for GFP imaging. The documentation was facilitated by a SPOT RT-slider digital camera connected to the microscope. Fluorescein isothiocyanate filters on the microscope were used to provide the GFP excitation. To confirm the nuclear localization, the transgenic and control plants were stained with DAPI as described (Devaiah et al., 2009).

RSA Analysis

The seedlings grown on P+ and P− media were spread out on petri plates and scanned at 200 dots per inch using a desktop scanner (UMAX Powelook 2100 XL). The lengths of the primary and lateral roots were measured using the ImageJ program (http://rsb.info.nih.gov/ij).

Determination of Shoot Area

Leaf area was measured by dissecting the leaves from the shoot individually and spreading them on agar plates. These plates were then scanned at 200 dots per inch, and ImageJ was used to compute the leaf area.

Root Hair Measurements

Seven-day-old seedlings germinated on one-half-strength MS petri plates containing 1.5% (w/v) Suc and 1.2% (w/v) agar were transferred to P+ or P− media. Two days post transfer, root hairs within the 5-mm region from the root tip were captured using a stereomicroscope (Nikon SMZ-U) equipped with a digital camera. The number and length of the root hairs were determined using ImageJ (http://rsb.info.nih.gov/ij/).

Anthocyanin Estimation

Seedlings germinated on one-half-strength MS plates were harvested 4 d after germination and ground into fine powder with liquid nitrogen. About 100 mg of tissue was used for anthocyanin quantification as described (Lange et al., 1971).

Quantification of Total Pi

A modified U.S. Environmental Protection Agency method 365.2 was used to determine the total Pi content in the wild-type and transgenic lines. The seedlings raised in petri plates were harvested, and about 50 mg of fresh sample was transferred into a preweighed vial and oven dried. The dry weight of the samples was recorded before flaming them to ash and dissolving them in 100 μL of concentrated HCl. Sample dilutions were prepared by adding 10 μL of the sample from the previous step to 790 μL of water. A total of 200 μL of mixed reagent (4.8 mM NH_4MoO_4, 2.5 N H_2SO_4, and 35 mM ascorbic acid) was added to this diluted sample (800 μL), and the reaction was incubated at 45°C for 20 min. Appropriate standards were used to measure the total Pi content at A_{650}, and the values were expressed as total Pi mg^{-1} tissue dry weight.

Real-Time PCR

RNA extraction and subsequent real-time PCR were performed as described (Ramaiah et al., 2011). The primers used for the amplification of *AtERF070* and the GA biosynthetic genes are listed in Supplemental Table S1.

Statistical Analysis

The data generated were subjected to Student's *t* test, and different letters on the histograms indicate means that were statistically different at $P \leq 0.05$.

Sequence data from this article can be found in the GenBank/EMBL data libraries under accession number BT025618.1.

Supplemental Data

The following materials are available in the online version of this article.

Supplemental Table S1. List of primers used for real-time PCR.

Received October 24, 2013; accepted December 23, 2013; published January 6, 2014.

LITERATURE CITED

Baek D, Park HC, Kim MC, Yun DJ (2013) The role of Arabidopsis MYB2 in miR399f-mediated phosphate-starvation response. Plant Signal Behav **8:** e23488

Bari R, Datt Pant B, Stitt M, Scheible WR (2006) PHO2, microRNA399, and PHR1 define a phosphate-signaling pathway in plants. Plant Physiol **141:** 988–999

Bariola PA, MacIntosh GC, Green PJ (1999) Regulation of S-like ribonuclease levels in Arabidopsis: antisense inhibition of *RNS1* or *RNS2* elevates anthocyanin accumulation. Plant Physiol **119:** 331–342

Bates TR, Lynch JP (1996) Stimulation of root hair elongation in Arabidopsis thaliana by low phosphorus availability. Plant Cell Environ **19:** 529–538

Beck T, Hall MN (1999) The TOR signalling pathway controls nuclear localization of nutrient-regulated transcription factors. Nature **402:** 689–692

Boutilier K, Offringa R, Sharma VK, Kieft H, Ouellet T, Zhang L, Hattori J, Liu CM, van Lammeren AA, Miki BL, et al (2002) Ectopic expression of BABY BOOM triggers a conversion from vegetative to embryonic growth. Plant Cell **14:** 1737–1749

Bustos R, Castrillo G, Linhares F, Puga MI, Rubio V, Pérez-Pérez J, Solano R, Leyva A, Paz-Ares J (2010) A central regulatory system largely controls transcriptional activation and repression responses to phosphate starvation in Arabidopsis. PLoS Genet **6:** e1001102

Calderon-Vazquez C, Ibarra-Laclette E, Caballero-Perez J, Herrera-Estrella L (2008) Transcript profiling of Zea mays roots reveals gene responses to phosphate deficiency at the plant- and species-specific levels. J Exp Bot **59:** 2479–2497

Camacho-Cristóbal JJ, Rexach J, Conéjéro G, Al-Ghazi Y, Nacry P, Doumas P (2008) PRD, an Arabidopsis AINTEGUMENTA-like gene, is involved in root architectural changes in response to phosphate starvation. Planta **228:** 511–522

Chen YF, Li LQ, Xu Q, Kong YH, Wang H, Wu WH (2009) The WRKY6 transcription factor modulates *PHOSPHATE1* expression in response to low Pi stress in *Arabidopsis*. Plant Cell **21:** 3554–3566

Chen ZH, Nimmo GA, Jenkins GI, Nimmo HG (2007) BHLH32 modulates several biochemical and morphological processes that respond to Pi starvation in Arabidopsis. Biochem J **405:** 191–198

Clough SJ, Bent AF (1998) Floral dip: a simplified method for Agrobacterium-mediated transformation of *Arabidopsis thaliana*. Plant J **16:** 735–743

Dai X, Wang Y, Yang A, Zhang WH (2012) *OsMYB2P-1*, an R2R3 MYB transcription factor, is involved in the regulation of phosphate-starvation responses and root architecture in rice. Plant Physiol **159:** 169–183

del Pozo JC, Allona I, Rubio V, Leyva A, de la Peña A, Aragoncillo C, Paz-Ares J (1999) A type 5 acid phosphatase gene from Arabidopsis thaliana is induced by phosphate starvation and by some other types of phosphate mobilising/oxidative stress conditions. Plant J **19:** 579–589

Devaiah BN, Karthikeyan AS, Raghothama KG (2007a) WRKY75 transcription factor is a modulator of phosphate acquisition and root development in Arabidopsis. Plant Physiol **143:** 1789–1801

Devaiah BN, Madhuvanthi R, Karthikeyan AS, Raghothama KG (2009) Phosphate starvation responses and gibberellic acid biosynthesis are regulated by the MYB62 transcription factor in Arabidopsis. Mol Plant **2:** 43–58

Devaiah BN, Nagarajan VK, Raghothama KG (2007b) Phosphate homeostasis and root development in Arabidopsis are synchronized by the zinc finger transcription factor ZAT6. Plant Physiol **145:** 147–159

Dolan L (2001) The role of ethylene in root hair growth in *Arabidopsis*. J Plant Nutr Soil Sci **164:** 141–145

Dubouzet JG, Sakuma Y, Ito Y, Kasuga M, Dubouzet EG, Miura S, Seki M, Shinozaki K, Yamaguchi-Shinozaki K (2003) *OsDREB* genes in rice, *Oryza sativa* L., encode transcription activators that function in drought-, high-salt- and cold-responsive gene expression. Plant J **33:** 751–763

Elliott RC, Betzner AS, Huttner E, Oakes MP, Tucker WQ, Gerentes D, Perez P, Smyth DR (1996) *AINTEGUMENTA*, an *APETALA2*-like gene of *Arabidopsis* with pleiotropic roles in ovule development and floral organ growth. Plant Cell **8:** 155–168

Feng JX, Liu D, Pan Y, Gong W, Ma LG, Luo JC, Deng XW, Zhu YX (2005) An annotation update via cDNA sequence analysis and comprehensive profiling of developmental, hormonal or environmental responsiveness of the Arabidopsis AP2/EREBP transcription factor gene family. Plant Mol Biol **59:** 853–868

Franco-Zorrilla JM, González E, Bustos R, Linhares F, Leyva A, Paz-Ares J (2004) The transcriptional control of plant responses to phosphate limitation. J Exp Bot **55:** 285–293

Fu X, Harberd NP (2003) Auxin promotes Arabidopsis root growth by modulating gibberellin response. Nature **421:** 740–743

Fujii H, Chiou TJ, Lin SI, Aung K, Zhu JK (2005) A miRNA involved in phosphate-starvation response in *Arabidopsis*. Curr Biol **15:** 2038–2043

Gu YQ, Yang C, Thara VK, Zhou J, Martin GB (2000) *Pti4* is induced by ethylene and salicylic acid, and its product is phosphorylated by the Pto kinase. Plant Cell **12:** 771–786

Hammond JP, Broadley MR, White PJ (2004) Genetic responses to phosphorus deficiency. Ann Bot (Lond) **94:** 323–332

Hobert O (2004) Common logic of transcription factor and microRNA action. Trends Biochem Sci **29:** 462–468

Hobert O (2008) Gene regulation by transcription factors and microRNAs. Science **319:** 1785–1786

Jain A, Nagarajan VK, Raghothama KG (2012) Transcriptional regulation of phosphate acquisition by higher plants. Cell Mol Life Sci **69:** 3207–3224

Jain A, Poling MD, Karthikeyan AS, Blakeslee JJ, Peer WA, Titapiwatanakun B, Murphy AS, Raghothama KG (2007a) Differential effects of sucrose and auxin on localized phosphate deficiency-induced modulation of different traits of root system architecture in Arabidopsis. Plant Physiol **144:** 232–247

Jain A, Poling MD, Smith AP, Nagarajan VK, Lahner B, Meagher RB, Raghothama KG (2009) Variations in the composition of gelling agents affect morphophysiological and molecular responses to deficiencies of phosphate and other nutrients. Plant Physiol **150:** 1033–1049

Jain A, Vasconcelos MJ, Sahi SV, Raghothama KG (2007b) Molecular mechanisms of plant adaptation to phosphate deficiency. *In* J Janick, ed, Plant Breeding Reviews, Vol 29. John Wiley & Sons, Hoboken, NJ, pp 359–419

Jiang C, Gao X, Liao L, Harberd NP, Fu X (2007) Phosphate starvation root architecture and anthocyanin accumulation responses are modulated by the gibberellin-DELLA signaling pathway in Arabidopsis. Plant Physiol **145:** 1460–1470

Karthikeyan AS, Varadarajan DK, Mukatira UT, D'Urzo MP, Damsz B, Raghothama KG (2002) Regulated expression of Arabidopsis phosphate transporters. Plant Physiol **130:** 221–233

Kobayashi T, Ogo Y, Itai RN, Nakanishi H, Takahashi M, Mori S, Nishizawa NK (2007) The transcription factor IDEF1 regulates the response to and tolerance of iron deficiency in plants. Proc Natl Acad Sci USA **104:** 19150–19155

Lange H, Shropshire W Jr, Mohr H (1971) An analysis of phytochrome-mediated anthocyanin synthesis. Plant Physiol **47:** 649–655

Lenburg ME, O'Shea EK (1996) Signaling phosphate starvation. Trends Biochem Sci **21:** 383–387

Lin SI, Chiang SF, Lin WY, Chen JW, Tseng CY, Wu PC, Chiou TJ (2008) Regulatory network of microRNA399 and *PHO2* by systemic signaling. Plant Physiol **147:** 732–746

Liu H, Yang H, Wu C, Feng J, Liu X, Qin H, Wang D (2009) Overexpressing HRS1 confers hypersensitivity to low phosphate-elicited inhibition of primary root growth in Arabidopsis thaliana. J Integr Plant Biol **51:** 382–392

López-Bucio J, Hernández-Abreu E, Sánchez-Calderón L, Nieto-Jacobo MF, Simpson J, Herrera-Estrella L (2002) Phosphate availability alters architecture and causes changes in hormone sensitivity in the Arabidopsis root system. Plant Physiol **129:** 244–256

López-Bucio J, Hernández-Abreu E, Sánchez-Calderón L, Pérez-Torres A, Rampey RA, Bartel B, Herrera-Estrella L (2005) An auxin transport independent pathway is involved in phosphate stress-induced root architectural alterations in Arabidopsis: identification of *BIG* as a mediator of auxin in pericycle cell activation. Plant Physiol **137:** 681–691

Lynch JP (2011) Root phenes for enhanced soil exploration and phosphorus acquisition: tools for future crops. Plant Physiol **156:** 1041–1049

Ma Z, Bielenberg DG, Brown KM, Lynch JP (2001) Regulation of root hair density by phosphorus availability in *Arabidopsis thaliana*. Plant Cell Environ **29:** 459–467

Marschner H (1995) Mineral Nutrition of Higher Plants. Academic Press, London

Martín AC, del Pozo JC, Iglesias J, Rubio V, Solano R, de La Peña A, Leyva A, Paz-Ares J (2000) Influence of cytokinins on the expression of phosphate starvation responsive genes in Arabidopsis. Plant J **24:** 559–567

Masucci JD, Schiefelbein JW (1994) The *rhd6* mutation of *Arabidopsis thaliana* alters root-hair initiation through an auxin- and ethylene-associated process. Plant Physiol **106:** 1335–1346

Misson J, Raghothama KG, Jain A, Jouhet J, Block MA, Bligny R, Ortet P, Creff A, Somerville S, Rolland N, et al (2005) A genome-wide transcriptional analysis using *Arabidopsis thaliana* Affymetrix gene chips determined plant responses to phosphate deprivation. Proc Natl Acad Sci USA **102:** 11934–11939

Miura K, Rus A, Sharkhuu A, Yokoi S, Karthikeyan AS, Raghothama KG, Baek D, Koo YD, Jin JB, Bressan RA, et al (2005) The Arabidopsis

SUMO E3 ligase SIZ1 controls phosphate deficiency responses. Proc Natl Acad Sci USA **102:** 7760–7765

Morcuende R, Bari R, Gibon Y, Zheng W, Pant BD, Bläsing O, Usadel B, Czechowski T, Udvardi MK, Stitt M, et al (2007) Genome-wide reprogramming of metabolism and regulatory networks of Arabidopsis in response to phosphorus. Plant Cell Environ **30:** 85–112

Muchhal US, Pardo JM, Raghothama KG (1996) Phosphate transporters from the higher plant *Arabidopsis thaliana*. Proc Natl Acad Sci USA **93:** 10519–10523

Müller R, Morant M, Jarmer H, Nilsson L, Nielsen TH (2007) Genome-wide analysis of the Arabidopsis leaf transcriptome reveals interaction of phosphate and sugar metabolism. Plant Physiol **143:** 156–171

Ogawa N, Saitoh H, Miura K, Magbanua JP, Bun-ya M, Harashima S, Oshima Y (1995) Structure and distribution of specific *cis*-elements for transcriptional regulation of PHO84 in *Saccharomyces cerevisiae*. Mol Gen Genet **249:** 406–416

Olszewski N, Sun TP, Gubler F (2002) Gibberellin signaling: biosynthesis, catabolism, and response pathways. Plant Cell (Suppl) **14:** S61–S80

O'Rourke JA, Yang SS, Miller SS, Bucciarelli B, Liu J, Rydeen A, Bozsoki Z, Uhde-Stone C, Tu ZJ, Allan D, et al (2013) An RNA-Seq transcriptome analysis of orthophosphate-deficient white lupin reveals novel insights into phosphorus acclimation in plants. Plant Physiol **161:** 705–724

Plaxton WC, Tran HT (2011) Metabolic adaptations of phosphate-starved plants. Plant Physiol **156:** 1006–1015

Raghothama KG (1999) Phosphate acquisition. Annu Rev Plant Physiol Plant Mol Biol **50:** 665–693

Ramaiah M, Jain A, Baldwin JC, Karthikeyan AS, Raghothama KG (2011) Characterization of the phosphate starvation-induced *glycerol-3-phosphate permease* gene family in Arabidopsis. Plant Physiol **157:** 279–291

Rausch C, Bucher M (2002) Molecular mechanisms of phosphate transport in plants. Planta **216:** 23–37

Ren F, Guo QQ, Chang LL, Chen L, Zhao CZ, Zhong H, Li XB (2012) Brassica napus PHR1 gene encoding a MYB-like protein functions in response to phosphate starvation. PLoS ONE **7:** e44005

Riechmann JL, Heard J, Martin G, Reuber L, Jiang C, Keddie J, Adam L, Pineda O, Ratcliffe OJ, Samaha RR, et al (2000) *Arabidopsis* transcription factors: genome-wide comparative analysis among eukaryotes. Science **290:** 2105–2110

Rubio V, Linhares F, Solano R, Martín AC, Iglesias J, Leyva A, Paz-Ares J (2001) A conserved MYB transcription factor involved in phosphate starvation signaling both in vascular plants and in unicellular algae. Genes Dev **15:** 2122–2133

Schwechheimer C, Bevan M (1998) Transcriptional regulation of plant gene expression. Trends Plant Sci **3:** 378–383

Shin H, Shin HS, Chen R, Harrison MJ (2006) Loss of At4 function impacts phosphate distribution between the roots and the shoots during phosphate starvation. Plant J **45:** 712–726

Shin H, Shin HS, Dewbre GR, Harrison MJ (2004) Phosphate transport in Arabidopsis: Pht1;1 and Pht1;4 play a major role in phosphate acquisition from both low- and high-phosphate environments. Plant J **39:** 629–642

Smith SE, Jakobsen I, Grønlund M, Smith FA (2011) Roles of arbuscular mycorrhizas in plant phosphorus nutrition: interactions between pathways of phosphorus uptake in arbuscular mycorrhizal roots have important implications for understanding and manipulating plant phosphorus acquisition. Plant Physiol **156:** 1050–1057

Stockinger EJ, Gilmour SJ, Thomashow MF (1997) *Arabidopsis thaliana CBF1* encodes an AP2 domain-containing transcriptional activator that binds to the C-repeat/DRE, a *cis*-acting DNA regulatory element that stimulates transcription in response to low temperature and water deficit. Proc Natl Acad Sci USA **94:** 1035–1040

Thibaud MC, Arrighi JF, Bayle V, Chiarenza S, Creff A, Bustos R, Paz-Ares J, Poirier Y, Nussaume L (2010) Dissection of local and systemic transcriptional responses to phosphate starvation in Arabidopsis. Plant J **64:** 775–789

Vance CP, Uhde-Stone C, Allan DL (2003) Phosphorus acquisition and use: critical adaptations by plants for securing a nonrenewable resource. New Phytol **157:** 423–447

Williamson LC, Ribrioux SPCP, Fitter AH, Leyser HMO (2001) Phosphate availability regulates root system architecture in Arabidopsis. Plant Physiol **126:** 875–882

Yamaguchi-Shinozaki K, Shinozaki K (2006) Transcriptional regulatory networks in cellular responses and tolerance to dehydration and cold stresses. Annu Rev Plant Biol **57:** 781–803

Yi K, Wu Z, Zhou J, Du L, Guo L, Wu Y, Wu P (2005) *OsPTF1*, a novel transcription factor involved in tolerance to phosphate starvation in rice. Plant Physiol **138:** 2087–2096

Zhou J, Jiao F, Wu Z, Li Y, Wang X, He X, Zhong W, Wu P (2008) *OsPHR2* is involved in phosphate-starvation signaling and excessive phosphate accumulation in shoots of plants. Plant Physiol **146:** 1673–1686